Supplementary Information

Unveiling the Synergy of Delocalized O 2*p* Holes and Localized Ce 4*f* States for Enhanced NH_3-SCR Activity on WO_3/La-CeO_2 Catalyst

Zi-Yi Guo[1], Zhi-Qiang Wang[1,*], and Xue-Qing Gong[2,*]

[1]State Key Laboratory of Green Chemical Engineering and Industrial Catalysis, Centre for Computational Chemistry and Research Institute of Industrial Catalysis, School of Chemistry and Molecular Engineering, East China University of Science and Technology, 130 Meilong Road, Shanghai 200237, China.

[2]State Key Laboratory of Synergistic Chem-Bio Synthesis, School of Chemistry and Chemical Engineering, Shanghai Jiao Tong University, 800 Dongchuan Road, Shanghai 200240, China.

*E-mails: zhiqiangwang@ecust.edu.cn; xqgong@sjtu.edu.cn

Additional figures

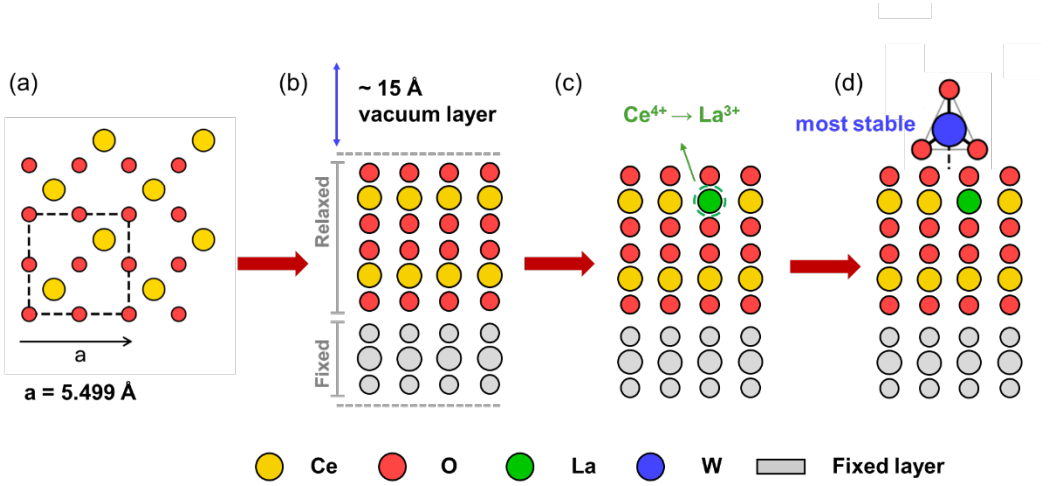

Scheme S1. Schematic illustration of the construction procedure for the WO_3/La-CeO_2(111) surface model. (a) Calculated structure of bulk CeO_2 unit cell (fluorite structure); (b) CeO_2(111) slab model (side view) containing three O-Ce-O tri-layers. The bottom O-Ce-O tri-layer is fixed (gray), and a vacuum layer region of ~15 Å is added; (c) La-doped CeO_2(111) slab model (side view) with a single La atom (green) substituting a surface Ce atom; (d) WO_3/La-CeO_2(111) surface with a tetrahedral WO_3 cluster deposited on the La-doped surface representing the most stable loading structure.

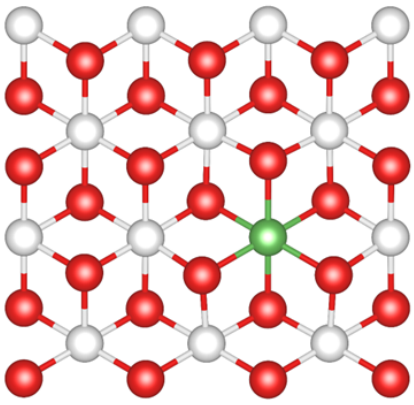

Figure S1. Calculated structure (top view) of La-CeO_2(111) surface. White: Ce, red: O, green: La, these notations are used throughout the paper.

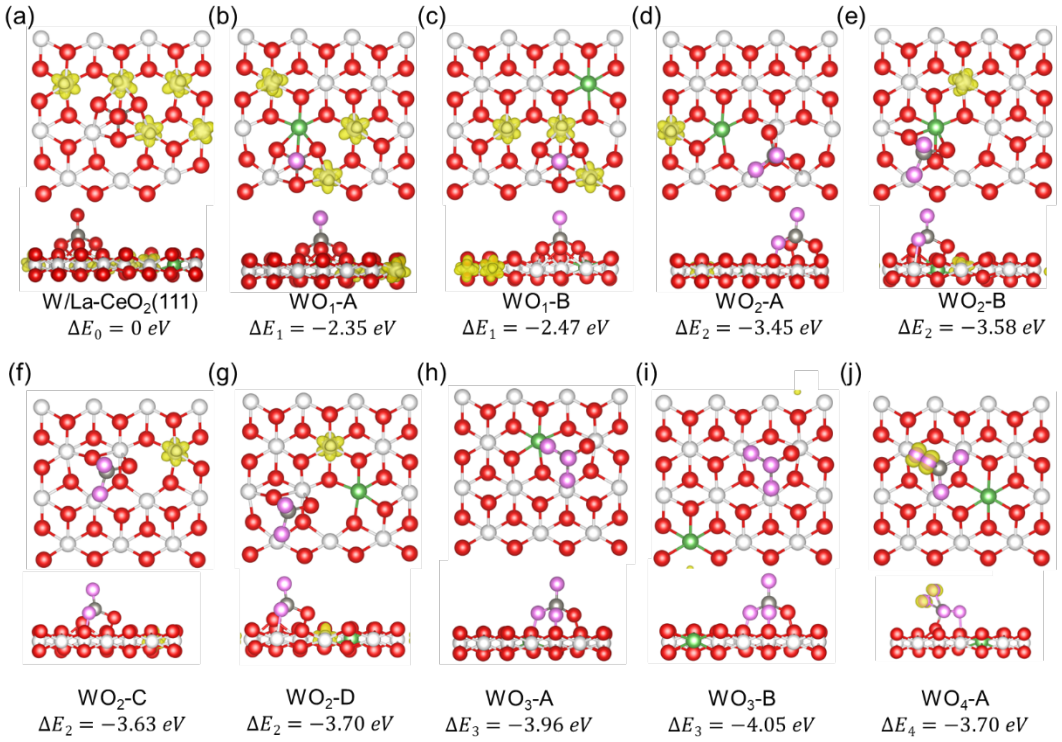

Figure S2. Calculated relative energies (ΔE_x, x = 0-4) and spin charge density differences (in yellow) of (a) W/La-CeO_2(111), (b-c) WO_1/La-CeO_2(111), (d-g) WO_2/La-CeO_2(111), (h-i) WO_3/La-CeO_2(111) and (j) WO_4/La-CeO_2(111) surfaces. The upper and lower panels show the top and side views, respectively. Grey: W, pink: O of WO_x, and these notations are used throughout the paper.

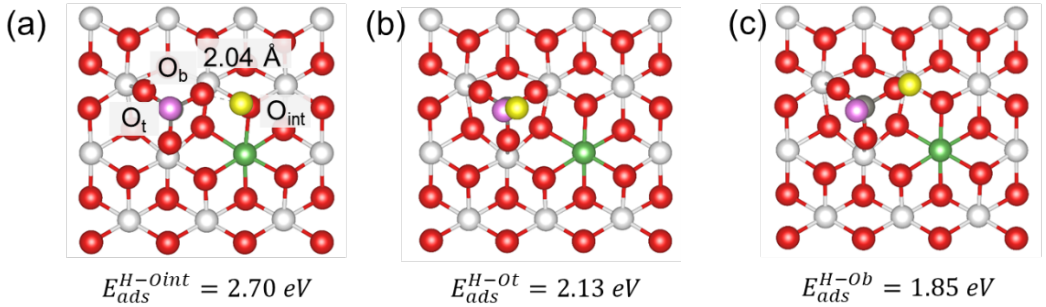

Figure S3. Calculated structures (top view) and adsorption energies of a single H at the O_{int}, O_t, and O_b sites on the WO_3/La-CeO_2(111) surface. Yellow: H atoms, pink: O of WO_x, these notations are used throughout the paper.

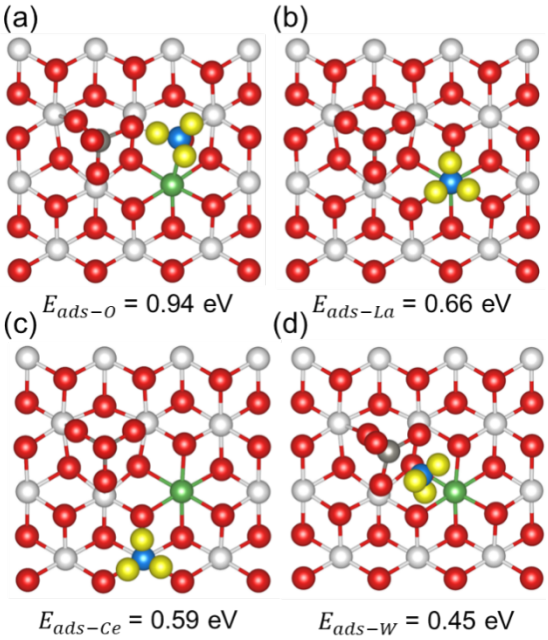

Figure S4. Calculated structures (top view) and adsorption energies of NH_3 adsorbed at different sites on the WO_3/La-CeO_2(111) surface. Blue: N atoms, these notations are used throughout the paper.

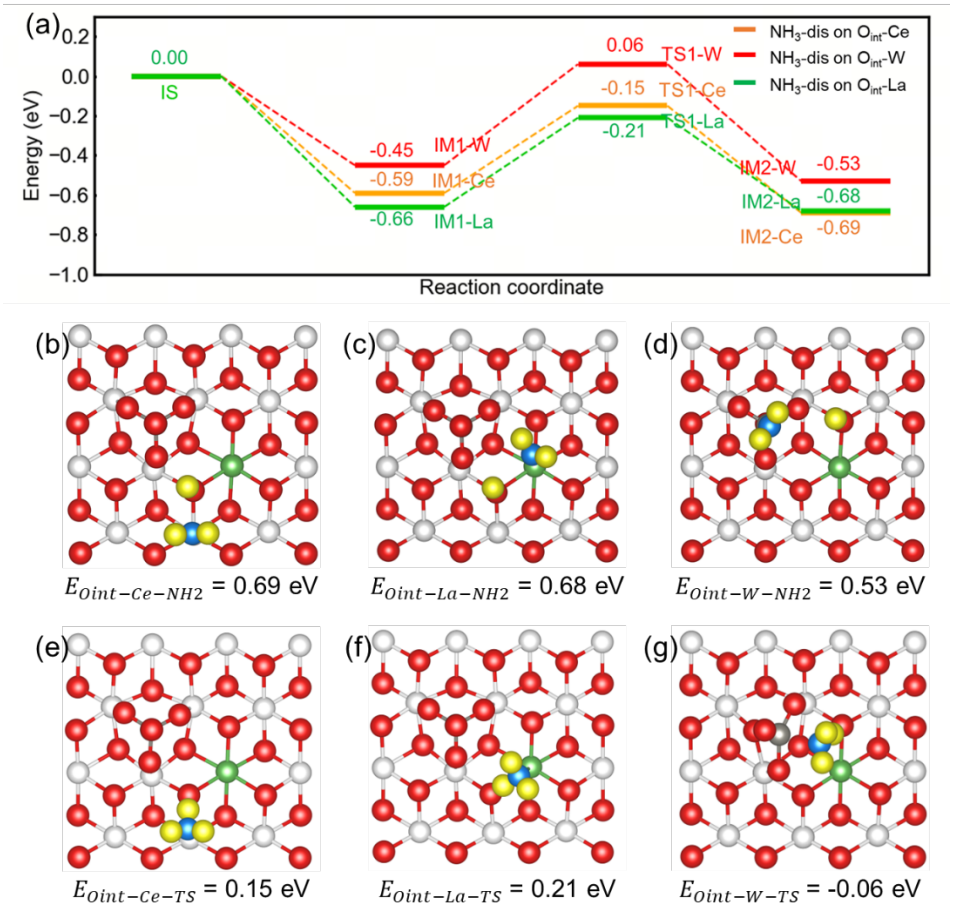

$E_{Oint-Ce-NH2}$ = 0.69 eV $E_{Oint-La-NH2}$ = 0.68 eV $E_{Oint-W-NH2}$ = 0.53 eV

$E_{Oint-Ce-TS}$ = 0.15 eV $E_{Oint-La-TS}$ = 0.21 eV $E_{Oint-W-TS}$ = -0.06 eV

Figure S5. (a) Calculated energy profiles for NH_3 dissociation at the O_{int}-Ce, O_{int}-La, and O_{int}-W sites on the WO_3/La-CeO_2(111) surface. (b-g) Calculated adsorption energies and key structures (top view) of the transition states and intermediates during the NH_3 dissociation at the O_{int}-Ce, O_{int}-La, and O_{int}-W sites on the WO_3/La-CeO_2(111) surface. This figure complements Figure 3 by presenting the energy profiles and key structures of alternative NH_3 dissociation pathways at different M-O sites on the WO_3/La-CeO_2(111) surface.

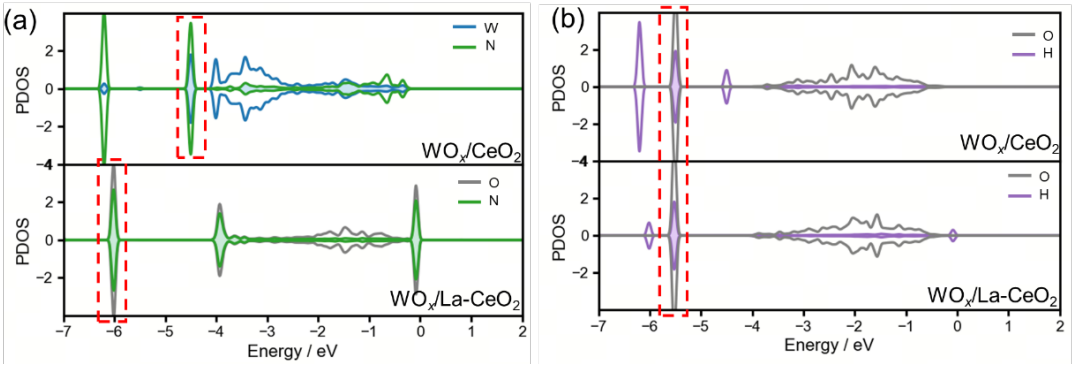

Figure S6. (a) Calculated projected DOS (PDOS) of the NH_2* species in the final states of NH_3 dissociation at W-O on the WO_3/CeO_2 surface and O_{int}-O_b sites on the WO_3/La-CeO_2 surface. (b) Calculated projected DOS (PDOS) of the O-H* species in the final states of NH_3 dissociation at W-O on the WO_3/CeO_2 surface and O-O sites on the WO_3/La-CeO_2 surface. All PDOSs were aligned with respect to the 2*s* energy level of the fixed oxygen in the slab.

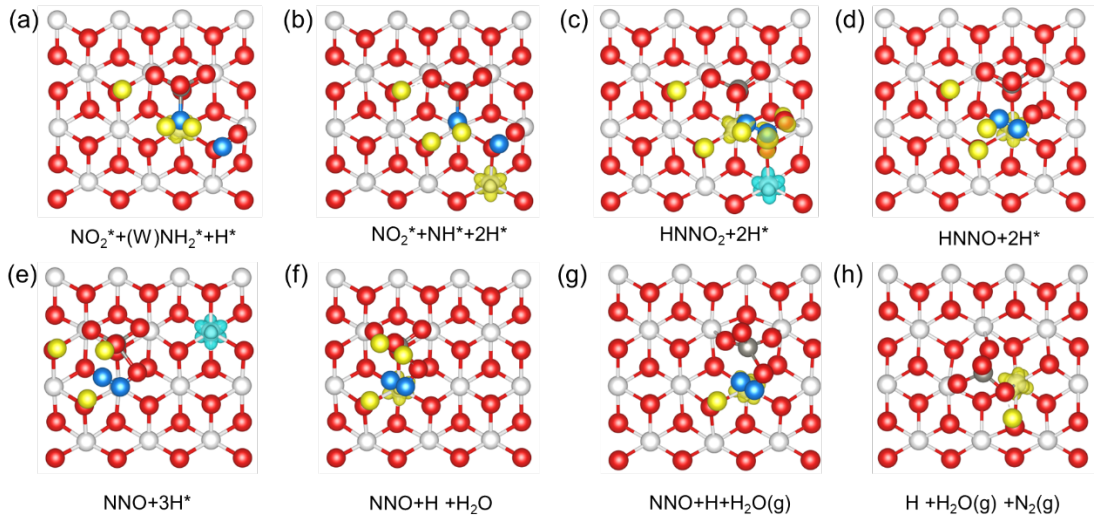

Figure S7. Calculated structures (top view) of key intermediates along NH_3-SCR pathway on the WO_3/CeO_2(111) surface.

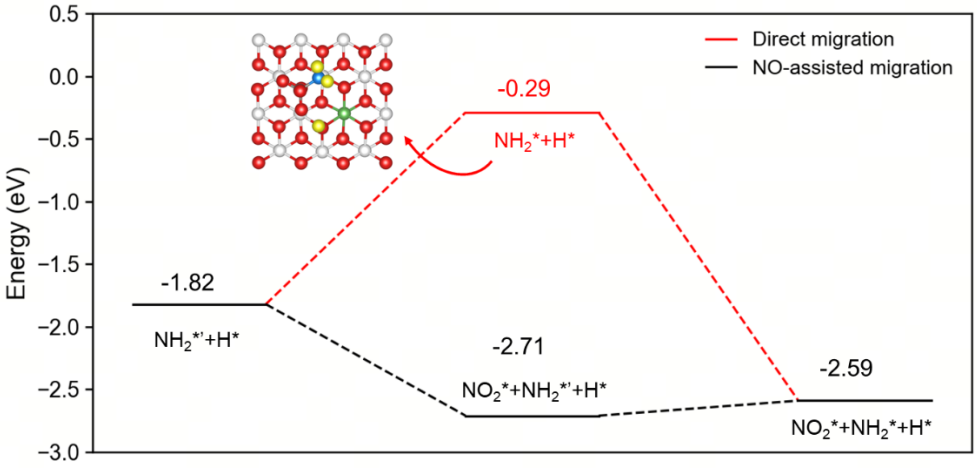

Figure S8. Calculated reaction energy profiles for two NH_2* migration pathways to the WO_x cluster site, *i.e.*, the direct pathway (red) and the NO-assisted pathway (black).

Table S1. Convergence tests of key computational parameters (cutoff energy, *k*-point mesh, slab thickness) using the NH_3 adsorption energy (E_{ads}, eV) at the O_{int} site on the WO_3/La-CeO_2(111) surface as a benchmark.

Parameter	Setting	E_{ads} (eV)	ΔE_{ads} (eV)
Cutoff energy	400 eV (this work)	0.94	-
	450 eV	0.94	0.00
	500 eV	0.94	0.00
K-point mesh	1 × 1 × 1 (Γ-point)	0.90	0.04
	2 × 2 × 1 (this work)	0.94	-
	3 × 3 × 1	0.94	0.00
Slab thickness	3 O-Ce-O tri-layers (this work)	0.94	-
	4 O-Ce-O tri-layers	0.94	0.00
	5 O-Ce-O tri-layers	0.95	0.01

Table S2. Calculated Ce/La-O bond lengths on the CeO_2(111) and La-CeO_2(111) surfaces. The listed values correspond to the seven coordinated O atoms around the cation center, including six lateral O atoms and one subsurface O atom.

Surface	Bond lengths / Å	Average length / Å
CeO_2(111)	2.37/2.37/2.37/2.37/2.37/2.37/2.37	2.37
La-CeO_2(111)	2.51/2.46/2.50/2.46/2.51/2.45/2.51	2.49

Table S3. Calculated *s*- and *p*-resolved integrated projected density of states (IPDOS) of lattice oxygen on the $CeO_2(111)$, La-$CeO_2(111)$, $WO_3/CeO_2(111)$, WO_3/La-$CeO_2(111)$ and WO_4/La-$CeO_2(111)$ surfaces.

	$N_{Olat,s}^{occ}$ / |e|	$N_{Olat,s}^{unocc}$ / |e|	$N_{Olat,p}^{occ}$ / |e|	$N_{Olat,p}^{unocc}$ / |e|
$CeO_2(111)$	153.32	0.38	330.74	4.66
La-$CeO_2(111)$	153.34	0.38	329.44	5.50
$WO_3/CeO_2(111)$	153.54	0.38	330.68	5.04
WO_3/La-$CeO_2(111)$	153.41	0.39	328.28	5.90
WO_4/La-$CeO_2(111)$	153.30	0.39	328.30	5.69

Table S4. Calculated Bader charges of the W species on the WO_{1-4}/La-$CeO_2(111)$ surfaces, and the Bader charges of O in the O_2 dimer on the WO_4/La-$CeO_2(111)$ surface are also shown.

	W Bader |e|	**O in O_2 dimer |e|**
WO_1/La-$CeO_2(111)$	2.69	/
WO_2/La-$CeO_2(111)$	2.68	/
WO_3/La-$CeO_2(111)$	2.68	/
WO_4/La-$CeO_2(111)$	2.68	-0.35

Table S5. Calculated adsorption energies of one H atom at different O sites on the $WO_3/CeO_2(111)$[1] and WO_3/La-$CeO_2(111)$ surfaces.

	E_{ads} (eV)		
	H-O_{int}	**H-O_t**	**H-O_b**
$WO_3/CeO_2(111)$	1.30	0.66	0.38
WO_3/La-$CeO_2(111)$	2.70	2.13	1.85

Table S6. Calculated site- and orbital-resolved integrated projected density of states (IPDOS) for lattice O (s, p), W (d), Ce (f), La (d) on the WO_3/La-$CeO_2(111)$ surface as well as for H adsorbed at the O_{int}, O_t, and O_b sites of WO_3/La-$CeO_2(111)$.

	$N^{occ}_{Olat,s}$ / |e|	$N^{unocc}_{Olat,s}$ / |e|	$N^{occ}_{Olat,p}$ / |e|	$N^{unocc}_{Olat,p}$ / |e|	$N^{occ}_{W,d}$ / |e|	$N^{unocc}_{W,d}$ / |e|	$N^{occ}_{Ce,f}$ / |e|	$N^{unocc}_{Ce,f}$ / |e|	$N^{occ}_{La,d}$ / |e|	$N^{unocc}_{La,d}$ / |e|
catalyst	153.41	0.39	328.28	5.90	3.41	0.05	33.04	364.80	0.57	0.02
H-O_{int}	153.44	0.39	330.68	5.55	3.42	0.14	33.33	371.68	0.57	0.02
	(0.02)	(0.00)	**(2.39)**	**(-0.35)**	(0.01)	(0.09)	(0.28)	(6.88)	(0.00)	(0.00)
H-O_t	153.34	0.39	331.03	5.59	3.46	0.09	33.34	372.06	0.57	0.02
	(-0.07)	(0.00)	**(2.75)**	**(-0.32)**	(0.05)	(0.04)	(0.30)	(7.26)	(0.00)	(0.00)
H-O_b	153.34	0.40	331.00	5.59	3.41	0.07	33.29	372.27	0.58	0.02
	(-0.07)	(0.01)	**(2.72)**	**(-0.32)**	(0.00)	(0.01)	(0.25)	(7.47)	(0.01)	(0.00)

References

[1] Z. Guo, C. Chen, K. C. Szeto, M. Taoufik, Z. Wang, X. Gong, Oxygen and Electron Storage Effects in W-Modified Ceria Catalysts for Ammonia Conversion, *Small*, 2024, **20**, 2406818.